Journal of Molecular Graphics and Modelling 29 (2010) 573–580

Contents lists available at ScienceDirect

Journal of Molecular Graphics and Modelling

journal homepage: www.elsevier.com/locate/JMGM

Computational approach to ensure the stability of the favorable ATP binding site in *E. coli* Hfq

Prettina Lazar, Songmi Kim, Yuno Lee, Keun Woo Lee*

Division of Applied Life Science (BK21 Program), Environmental Biotechnology National Core Research Center (EB-NCRC), Plant Molecular Biology and Biotechnology Research Center (PMBBRC), Gyeongsang National University (GNU), 900 Gazwa-dong, Jinju 660-701, Republic of Korea

ARTICLE INFO

Article history:
Received 10 September 2010
Received in revised form 1 November 2010
Accepted 5 November 2010
Available online 11 November 2010

Keywords:
Host factor protein-Hfq
ATP
Oligoribonucleotide
RNA
Post-transcriptional regulation
Molecular dynamics simulation
Mutation
Aromatic stacking
Destabilization

ABSTRACT

Bacterial Hfq is a highly conserved thermostable protein of about 10 kDa. The Hfq protein was discovered in 1968 as an *E. coli* host factor that was essential for replication of the bacteriophage Qβ. It is now clear that Hfq has many important physiological roles. In *E. coli*, Hfq mutants show a multiple stress response related phenotypes. Hfq is now known to regulate the translation of two major stress transcription factors RpoS and RpoE in Enterobacteria and mediates its plieotrophic effects through several mechanisms. It interacts with regulatory sRNA and facilitates their antisense interaction with their targets. It also acts independently to modulate mRNA decay and in addition acts as a repressor of mRNA translation. Recent paper from Arluison et al. [9] provided the first evidence indicating that Hfq is an ATP-binding protein. They determined a plausible ATP-binding site in Hfq and tested Hfq's ATP-binding affinity and stoichiometry. Experimental data suggest that the ATP-binding by the Hfq–RNA complex results in its significant destabilization of the protein and the result also proves important role of Tyr25 that flanks the cleft and stabilizes the adenine portion of ATP, possibly via aromatic stacking. In our study, the ATP molecule was docked into the predicted binding cleft using GOLD docking software. The binding nature of ATP and its effect on Hfq–RNA complex was studied using molecular dynamics simulations. Importance of Tyr25 residue was monitored and revealed using mutational study on the modeled systems. Our data and the corresponding results point to one of Hfq functional structural consequences due to ATP binding and Tyr25Ala mutation.

1. Introduction

Hfq is an abundant RNA-binding protein in *E. coli* that is highly conserved and appears to function as a global regulator of gene expression. Intriguingly, Hfq has been reported to have ATPase activity, albeit it is relatively weak [1]. Sequence comparison between Hfq and the heat shock protein ClpB revealed some homology between the ATP binding site of ClpB and the stretch of the Hfq sequence that includes β2. This 'modified Walker A box' is rather open, and how and where ATP binds and the role of the ATPase activity are under investigation. It should be noted that the chaperone activities of Hfq are independent of ATP hydrolysis, thereby leaving the function of the ATPase activity of Hfq an open question [2]. Finally, Hfq was also recently reported to interact with both ribosomal proteins S1 and an RNA polymerase, to exhibit ATPase activity and to affect the polyadenylation of bacterial RNAs. Alternatively, it is also possible that stimulation of PAP I-dependent poly(A) synthesis is correlated with the ATPase activity of Hfq [3,4]. Hfq is known to associate with the ribosomal protein S1 to promote replication of the RNA phage Qβ [5]. Hfq and S1 have also been found to associate with RNA polymerase, and an ATPase activity was found for Hfq, although no catalytic site is obvious from the sequence or crystal structures. If Hfq either has an ATPase activity or associates with an ATPase, such an ATPase might help remodel RNAs as they anneal and could provide external energy for reactions such as strand displacement [6]. Biochemical and genetic evidence suggests that the ATPase activity is an intrinsic activity of Hfq rather than that of an Hfq-associated protein. Hfq purified to apparent homogeneity shows ATPase activity. This finding suggests that at least some representatives of the extended family of eukaryotic Sm-like proteins (required for processes as diverse as pre-mRNA splicing, mRNA degradation and telomere formation) that share sequence homology with Hfq are also ATPases. There is limited sequence homology between Hfq and known ATP-utilizing enzymes, and in fact, Hfq belongs to new class of ATPases named AAA^+, which is a class of chaperone-like ATPases associated with the assembly, operation, and disassembly of protein complexes [7,8]. The hexameric structure of Hfq is quite similar to those of

* Corresponding author. Tel.: +82 55 751 6276; fax: +82 55 752 7062.
E-mail address: kwlee@gnu.ac.kr (K.W. Lee).

1093-3263/$ – see front matter © 2010 Published by Elsevier Inc.
doi:10.1016/j.jmgm.2010.11.003

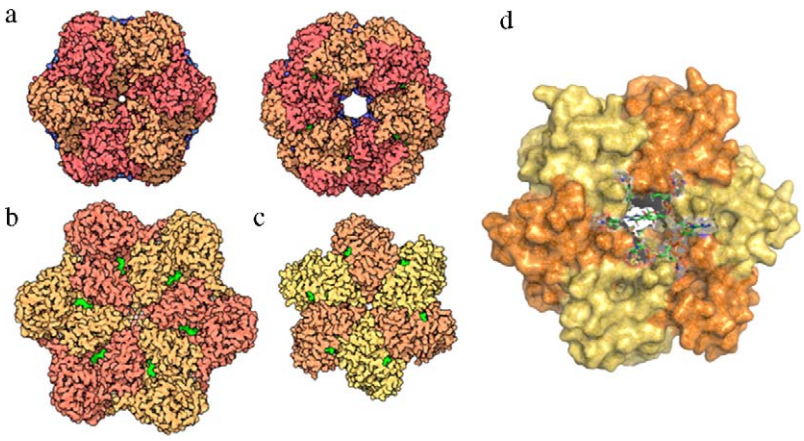

Fig. 1. Structural comparison of Hfq with three known examples of AAA+ ATPases (a) HslUV, (b) p97, (c) T antigen and (d) Hfq.

known AAA+ ATPases like HslUV, p97 and T Antigen, and hence the probable ATP binding site in Hfq must be similar to that of the known AAA+ ATPases (Fig. 1).

Using a combination of biochemical and genetic techniques, a plausible ATP-binding site was identified in Hfq and Hfq's ATP-binding affinity and stoichiometry were tested. The results of RNA footprinting and binding analyses suggest that ATP binding by the Hfq–RNA complex results in its significant destabilization. RNA footprinting indicates deprotection of Hfq-bound RNA tracts in the presence of ATP, suggestive of their release by the protein. Moreover, author mentioned that a Y25A mutation resulted in a near-knockout of ATP hydrolysis in the purified protein [9].

Computational approaches like molecular docking simulations, molecular modeling and molecular dynamics simulations were used to look for the most stable and favorable ATP binding site and any significant effects of ATP on the structure or stability of the Hfq–RNA complex. The importance of Tyr25 was also assessed by hexamutant analysis of Hfq. An attempt was made to substantiate the microscopic and atomic details of Arluison's experimental results with our study. These types of studies will address where it is that ATP comfortably binds on Hfq and characterize the influence of Hfq's ATPase activity on the six-fold symmetry and conformation of the Hfq–RNA complex.

2. Materials and methods

2.1. Molecular docking simulation

Binding interactions can be ascertained by docking inhibitors into the active site of a protein. The GOLD 3.01 [10] program was used to find a stable ATP binding mode along the boundary between individual Hfq subunits. It employs genetic algorithm in which information about the conformation of the ligand and hydrogen bonding is encoded into a chromosome. GOLD considers complete ligand flexibility and partial protein flexibility, and the energy functions are partly based on conformational and non-bonded interactions. Several types of scoring functions such as GoldScore, ChemScore and User-defined score are available. The following default genetic algorithm parameters were used: population size, 30; 1.1 for selection, number of islands, 5; number of genetic operations, 100,000; and niche size, 2. A pseudo-atom was created at the center of the interface gap between two adjacent monomers (chain A and chain B) of *E. coli* Hfq, and the active site was defined as 10 Å around it. The GoldScore was adopted to rank the docked conformations of a single ATP molecule between the two subunits of *E. coli* Hfq.

2.2. System set-up using molecular modeling

Using the selected conformation of ATP docked with two Hfq subunits, an Hfq hexamer with six individual ATP molecules docked along the boundaries of pairs of Hfq subunits was modeled and prepared by superimposition. Similarly, a structure of *E. coli* Hfq in the RNA-binding conformation (PDB ID: 1HK9) [11] was adopted from the only available crystal structure of *S. aureus* Hfq (PDB ID: 1KQ2) [12] with AU_5G. In *E. coli*, the oligo-ribonucleotide was replaced with rA7 instead of AU_5G, because *E. coli* Hfq selectively binds to rA7. Four different conformations of wild-type *E. coli* Hfq systems were modeled, including: apo form Hfq, Hfq with bound RNA (rA7), Hfq with six bound ATP molecules, and Hfq bound to both ATP (6 molecules) and RNA (rA7). A hexamutant Hfq with the mutation Tyr25Ala was also modeled to study the importance of Tyr25. This hexamutant was modeled in the same four configurations mentioned above: apo form; with bound RNA (rA7); with bound ATP (6 molecules); and with RNA (rA7) + ATP (6 molecules). All the molecular modeling studies were carried out using Discovery Studio version 2.5 [13].

2.3. Computational details of the molecular dynamics simulations

The GROMACS package [14,15] was used to perform MD simulations, where the protein and water molecules were described by parameters from AMBER99 [16] and TIP3P [17] force fields, respectively. Hydrogen atoms were added and the protonation state of ionizable groups was chosen appropriately at pH 7.0. A cubic box of solvent 12 nm in length was generated to perform the simulations in an aqueous environment. Na^+ or Cl^- counter-ions were added by replacing water molecules to ensure the overall charge neutrality of the simulated system. The particle mesh Ewald (PME) method was applied to accurately determine the long-range electrostatic interactions [18]. A grid spacing of 1.2 Å was used for fast Fourier transform calculations and van der Waals interactions were considered by applying a cutoff of 9 Å. Aconstant temperature and pressure (300 K and 1 bar) was maintained with a Berendsen thermostat [19] and a Parrinello–Rahman [20] barostat. The systems were subjected to the steepest descent energy minimization process with a tolerance of 1000 kJ/mol. The time step for the simulations was set to 2 fs. During the system equilibration process, the protein backbone was frozen and the solvent molecules with counterions were allowed to move for 100 ps under NPT conditions at 300 K. The equilibrated structure was then used for the following 5-ns production runs. Bonds between heavy atoms and corresponding hydrogen atoms were constrained to their equilib-

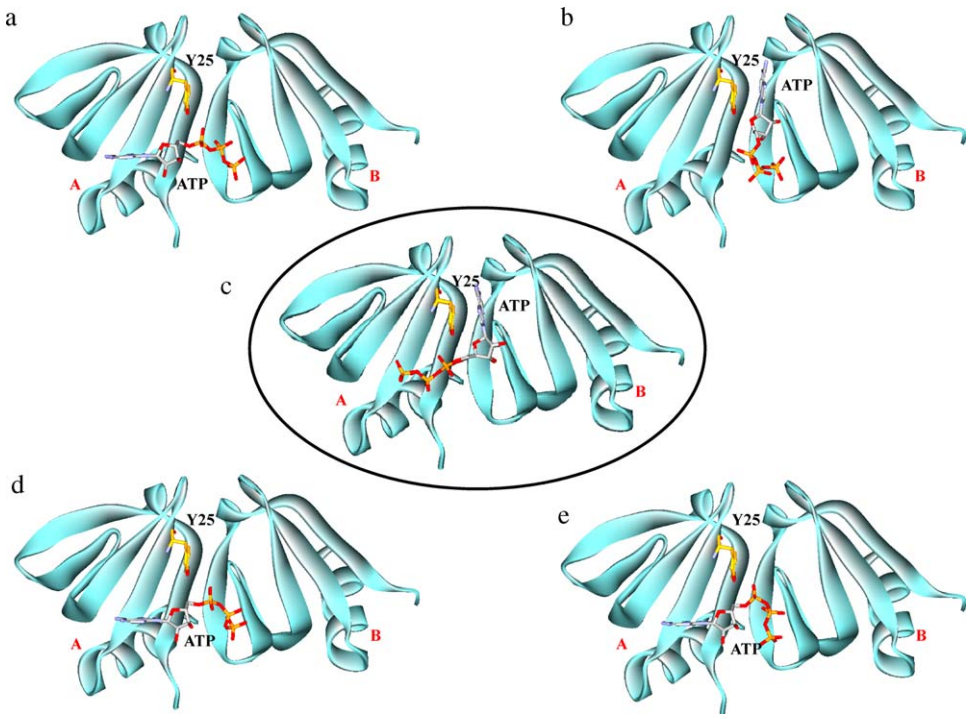

Fig. 2. Molecular docking simulations results of top 5 ranked poses of the ATP bound between two of the Hfq monomers (chain A and chain B) shown in blue ribbon style with Tyr25 and ATP shown in stick model, coloured by atom (a) Pose-18, (b) Pose-12, (c) Pose-15, (d) Pose-2 and (e) Pose-1. The encircled one shows the chosen binding pose of ATP with Hfq monomers. (For interpretation of the references to color in this figure legend, the reader is referred to the web version of the article.)

rium bond lengths using the LINCS algorithm [21,22]. During the production phase, the coordinate data were written to the file every 10 ps.

2.4. Model structure setup for simulation

We considered eight modeled conformations in our study: both wild-type Hfq and a hexamutant version (Y25A) were modeled in apo form, bound to RNA, bound to ATP, and bound to both ATP and RNA. A detailed summary of the different model systems is listed in Table 1.

Table 1
System details for the four wild type and hexamutant Hfq systems respectively for molecular dynamics simulations study.

No.	System details	No. of TIP3P water added	No. of Cl^- ion added
1	Hfq (apo)	22,037	24
2	Hfq + RNA	21,176	18
3	Hfq + ATP	21,988	12
4	Hfq + ATP + RNA	21,121	6
5	Hfq(Y25A)	22,060	24
6	Hfq(Y25A) + RNA	21,192	18
7	Hfq(Y25A) + ATP	21,991	12
8	Hfq(Y25A) + ATP + RNA	21,126	6

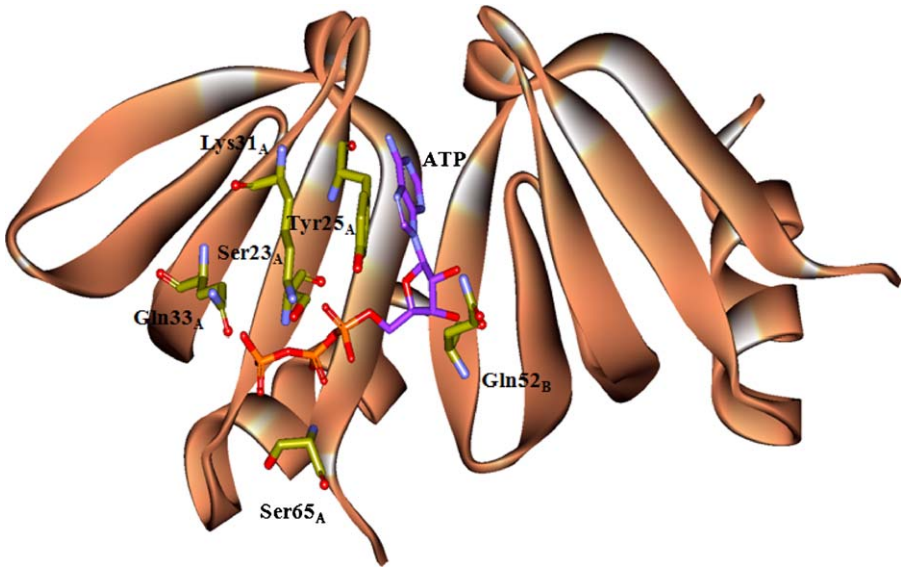

Fig. 3. Selected docked Pose-15 of ATP at the binding site Hfq, showing the key interacting residues.

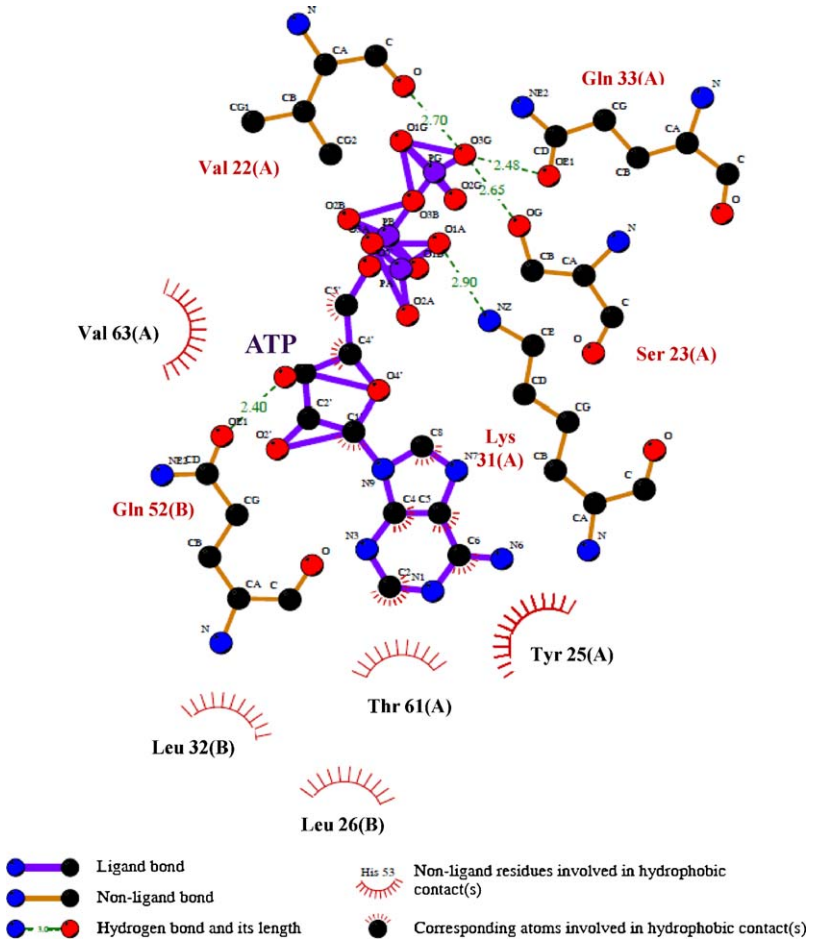

Fig. 4. Protein–ligand interaction 2D map of Hfq and ATP using LIGPLOT Program. Hydrogen bond forming residues were shown in lines with hydrogen bonds shown as dotted lines and residues interacting by hydrophobic interactions were represented as lines in red. (For interpretation of the references to color in this figure legend, the reader is referred to the web version of the article.)

3. Results and discussion

3.1. Molecular docking and validation

Docking studies were performed to gain insight into the most probable and stable binding conformation for ATP along the boundary of two Hfq subunits. A total of 30 different conformations were obtained, out of which the top five were selected to have their conformational stability assessed. The docking scores as evaluated by GOLD for the top five conformations are 68.47, 66.16, 64.46, 64.19 and 63.93, respectively, as presented in Table 2. The corresponding docking conformations of ATP bound between two monomers of Hfq (chain A and chain B) are clearly shown in Fig. 2.

The ATP-bound conformations were analyzed individually. Based on the binding mode analysis, conformation 15 (which is ranked 4th among the top 5) was selected as the best binding mode between ATP and the Hfq subunits, because this conformation was found to be compatible with the previous experimental and theoretical results and explains all the features of ATP-binding by Hfq [12]. Analyses of this Hfq–ATP binding conformation revealed favorable π–π stacking interactions involving the adenine ring of ATP and the phenyl ring of Tyr25 (Fig. 3). Five strong hydrogen bonding contacts with ATP were also observed with Val22, Lys31, Gln33 and Ser23 of chain A and Gln52 of chain B of Hfq (Fig. 4).

Ligplot analyses were introduced to elucidate the interaction between the docked ATP and the key interacting residues of chain

Table 2
List of top 5 poses with the corresponding GOLD fitness scores based on Molecular Docking Simulation studies.

S. No.	Ligand poses	GOLD fitness score
1	Pose-18	68.47
2	Pose-12	66.16
3	Pose-2	64.46
4	Pose-15	64.19
5	Pose-1	63.93

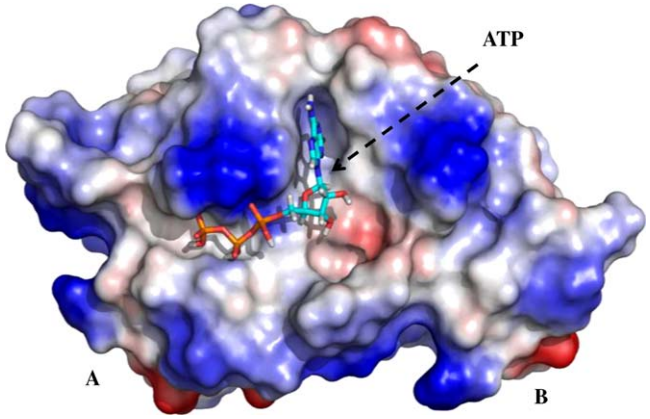

Fig. 5. Electrostatic surface diagram of Hfq showing the ATP binding cleft along the boundary of the two subunits (chain A and chain B) of Hfq.

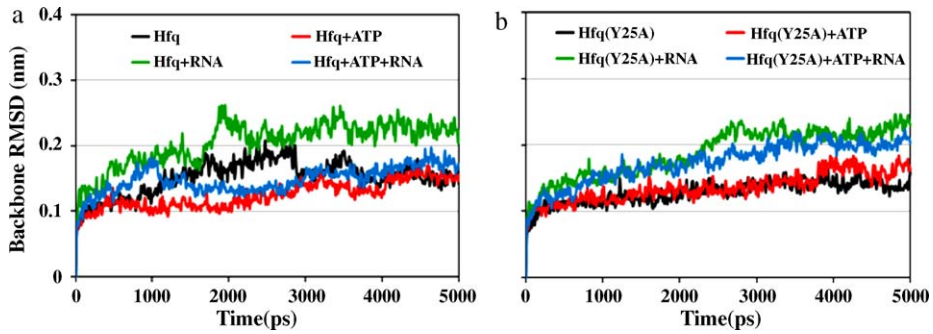

Fig. 6. Time dependence of the root mean square deviation (RMSD) for the protein backbone atoms during the simulation in Hfq modeled (a) wild type and (b) hexamutant systems.

A and B. Ligplot is an essential tool for understanding hydrophobic interactions as well as hydrogen bonding patterns [23]. The same H-bond interactions observed in the docking results were obtained with the Hfq–ATP bound conformation. In addition to the already known Tyr25, which provides favorable π–π stacking interactions with adenine ring of ATP, Thr61 and Val63 of chain A along with Leu26 and Leu32 of chain B were observed to undergo hydrophobic interactions with ATP. Thus, the Ligplot analyses were especially for revealing the hydrophobic interaction patterns. Very strong hydrophobic interactions were noticed between ATP and Hfq residues in chains A and B (Fig. 4). These strongly conserved residues form a composite binding site capable of providing a network of Hfq/ATP interactions that staple the nucleotide into this surface pocket. The electrostatic surface of the Hfq chains clearly show an ATP binding cleft, of the selected ATP-bound conformation from our docking study (Fig. 5).

3.2. Stability and compactness of the modeled hfq systems

To further investigate the individual and combined influences of ATP- and RNA-binding on the overall backbone of wild-type and hexamutant Hfq, RMSDs were calculated. During the simulation times, the RMSD of the protein backbone atoms reflects the stability of the modeled system. All the systems were stable during 5 ns MD simulations with both wild-type and hexamutant Hfq. Only the presence of RNA gave more than 0.2 nm of deviation in both types of Hfq system. With the other modeled Hfq systems, the RMSD values gradually increased until 1 ns, but they stabilized for the remainder of the 5 ns (Fig. 6).

To assess the compactness of the modeled systems, the radius of gyration was calculated during the course of the simulation. The six-fold ring symmetry of Hfq appeared to be the least compact in the hexamutant Hfq system with ATP and RNA together, which weakened the compactness of the Hfq hexamer compared to the other systems (Fig. 7). This change in compactness of system may

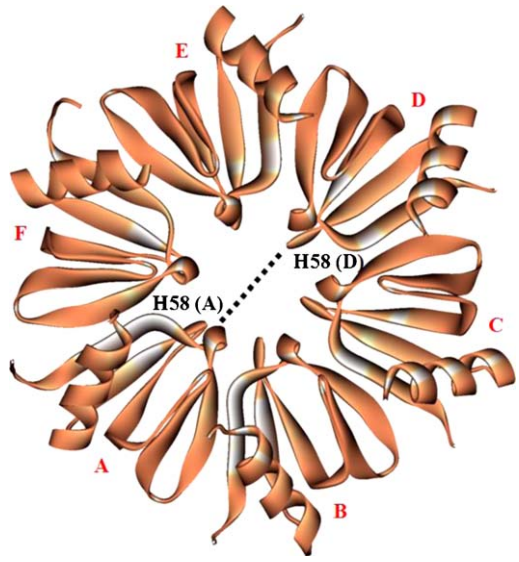

Fig. 8. Hfq protein with the selected pore lining residues His58 of chain A and chain D. Showing the pore diameter as dotted lines and chain names indicated in red colour. (For interpretation of the references to color in this figure legend, the reader is referred to the web version of the article.)

be due to some factors related to the mutation of the Tyr25 residue.

3.3. Differences in RNA pore diameter and H-bonds between Hfq–RNA and Hfq–ATP

The pore diameter of Hfq was examined because a specific pore diameter is required for RNA to thread through the pore for post-translational modification. The pore diameter was calculated by measuring the distance from the center of an atom of one of the pore-lining residues of the highly conserved YKHAI motif of one

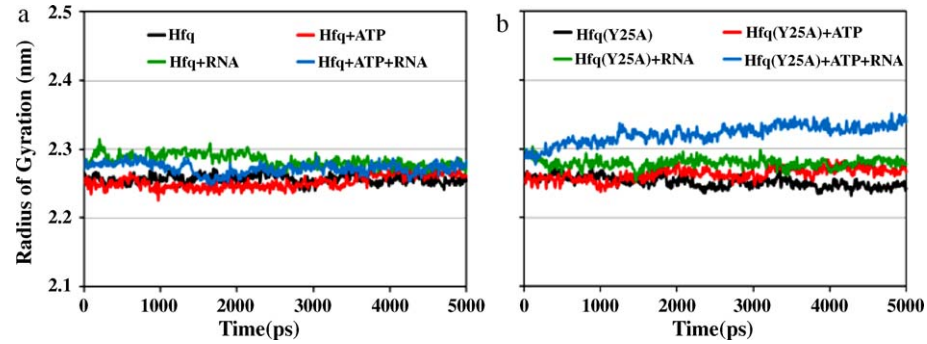

Fig. 7. Time dependence of the radius of gyration (Rg) for the protein atoms during the simulation in Hfq modelled (a) wild type and (b) hexamutant systems.

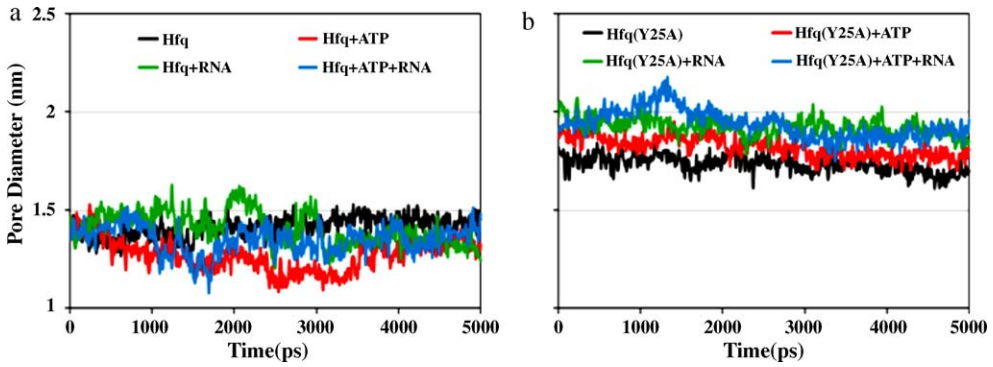

Fig. 9. Time dependence change in Hfq pore diameter for all the systems.

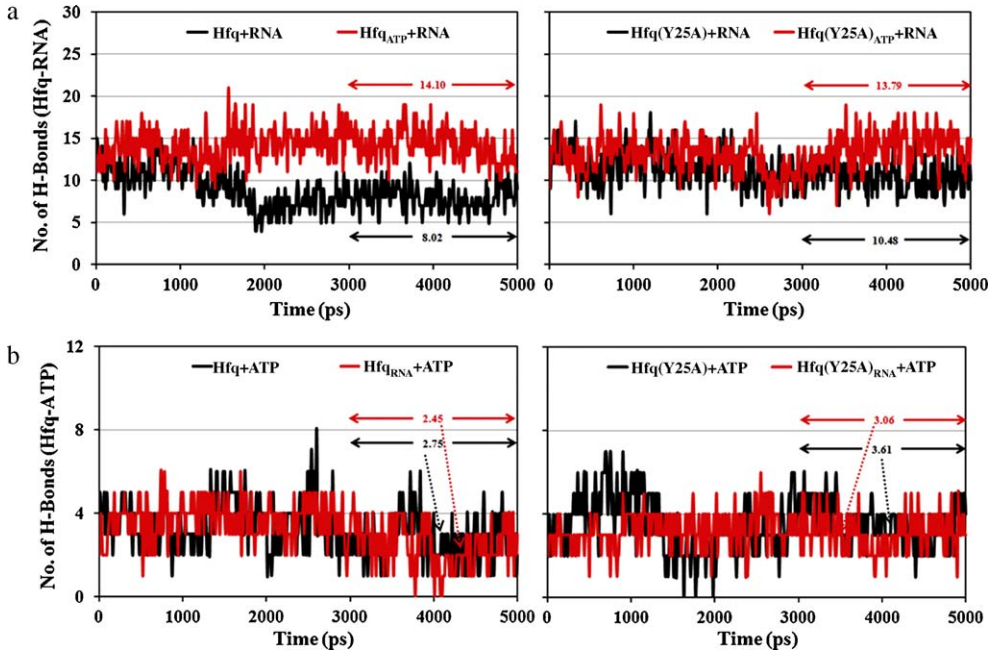

Fig. 10. Time dependence change in number of hydrogen bonding. (a) Changes in no. of H-bond between Hfq–RNA in absence and presence of ATP. (b) Changes in no. of H-bond between Hfq–ATP in absence and presence of RNA. The variances are shown with red and black dotted arrows. (For interpretation of the references to color in this figure legend, the reader is referred to the web version of the article.)

chain to the same pore-lining residue of the opposite chain. For this purpose, the two His58 residues in the YKHAI motifs of chains A and D were used (Fig. 8).

The pore diameter of the wild-type Hfq–RNA complex is 1.2–1.4 nm, but we found that the pore diameter increased to about 2 nm in all the hexamutant systems during the simulation (Fig. 9). This might be one of the reasons for the decrease in compactness of the hexamutant Hfq system with bound ATP and RNA, and it suggests that the hexamutation may alter the post-translational modification and, more specifically, the assembly/remodeling of RNA–protein complexes and, hence, the threading of RNA through the pore.

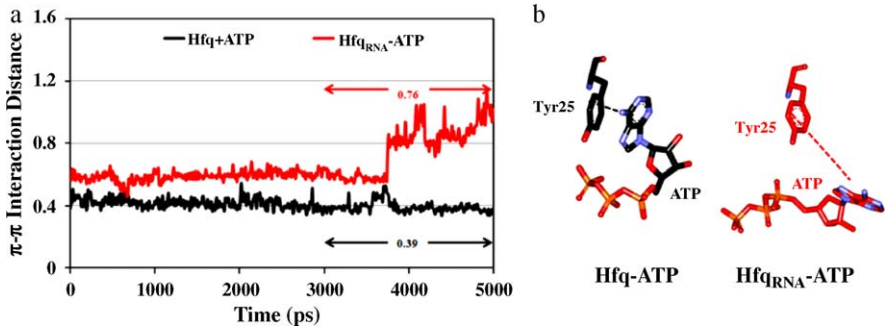

Fig. 11. Time dependence change in π–π interaction between the Tyr25 ring and the adenine part of ATP. (a) Shows π–π interaction distance in absence and presence of RNA in Hfq bound to ATP (b) Schematic representation of the π–π interaction distance between the Tyr25 ring and the adenine part of ATP (shown in stick model) both in absence and presence of RNA in Hfq bound to ATP.

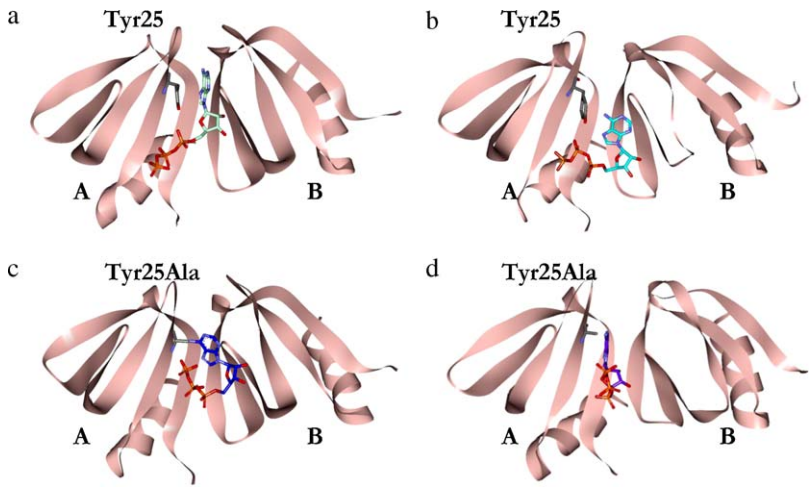

Fig. 12. ATP position orientations in average structure of different modeled systems during the simulation. (a) Hfq bound to ATP alone, (b) Hfq bound to ATP in presence of RNA, (c) mutant Hfq(Y25A) bound to ATP alone, (d) mutant Hfq(Y25A) bound to ATP in presence of RNA.

Hydrogen bonding analysis was carried out to assess the changes in the Hfq–RNA interaction in the absence and presence of ATP molecules. Similarly, the interaction between Hfq (only 2 subunits) and ATP (1 molecule) in the absence and presence of RNA were analyzed during the simulations. The analysis of Hfq–RNA interactions showed that the presence of ATP (Hfq_{ATP} + RNA) enhances the interaction of RNA with Hfq in the wild-type system, whereas the Hfq–RNA interaction is similarly strong and stable in the hexamutant system with or without ATP (Fig. 10a). Similarly, the analysis of Hfq–ATP interactions showed that the presence of RNA (Hfq_{RNA} + ATP) tends to affect ATP binding in the wild-type system. We observed that in presence of RNA, ATP loses its contact with Hfq at around 4 ns, whereas the hexamutant systems displayed no such effect (Fig. 10b).

3.4. Changes in the π–π stacking interaction between the phenyl ring of Tyr25 and adenine moiety of ATP

According to Arulison et al. [12], the ATP binding cleft in Hfq has favorable π–π stacking interactions between the phenyl ring of Tyr25 and the adenine moiety of ATP. The general structural effects on the Hfq hexamer of the absence/presence of RNA were assessed. The π–π interaction was analyzed by calculating the distance between the center of atom of the Tyr25 ring atoms and the adenine moiety atoms of ATP. This analysis showed that in the absence of RNA (Hfq + ATP), the π–π interaction between the Tyr25 ring and adenine ring of ATP is stable, whereas in the presence of RNA (Hfq_{RNA} + ATP), the π–π interaction totally vanishes after 4 ns (Fig. 11).

This result suggests that ATP binding does not induce a major structural change in Hfq (Fig. 12a). In contrast, in the presence of both RNA and ATP together, the six-fold symmetry of the Hfq ring is broken, thereby implying a major structural change (Fig. 12b). Interestingly, we detected no such change with Tyr25Ala Hfq, suggesting that the mutant protein is unable to undergo this conformational transition seen with wild-type Hfq (Fig. 12c and d). The orientation of the ATP binding site substantiates the experimental evidence and the results obtained so far in our study.

3.5. Changes in monomer aggregation in the different systems

The average van der Waal interaction energies between two monomer subunits of Hfq modeled systems were calculated to determine the aggregation between them with the conformation most similar to the averaged structure during the simulation time. The calculated average van der Waals energy for the Hfq system with both RNA and ATP was −49.723 kcal/mol, whereas for all the other systems the van der Waals energy ranged between ∼60 and ∼78 kcal/mol (Table 3). At −78.673 kcal/mol, the wild-type Hfq system has the most favorable van der Waals energy between monomers. Thus, the system with both RNA and ATP had the weakest van der Waals energy between the monomers among all the modeled wild-type and hexamutant systems (Fig. 13). This can be interpreted as weak aggregation between the Hfq monomers and, hence, a disruption of the six-fold symmetry of the Hfq ring structure as per Arluison et al. This correlates very well with the electron microscopic analyses of Hfq in the presence and absence of RNA and nucleotides in our modeled Hfq systems.

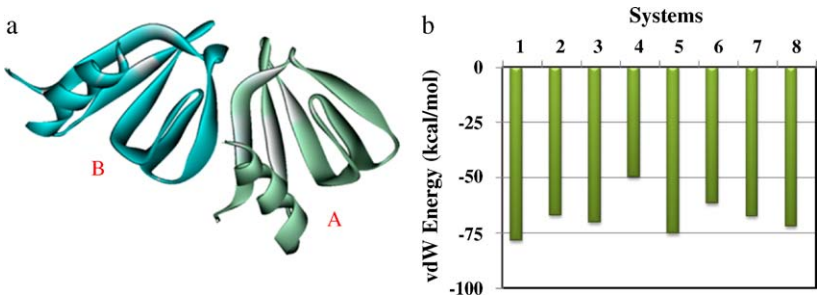

Fig. 13. Average van der Waals interaction energy calculations. (a) The two subunits utilized from the average structure of each systems and (b) bar graph of the vdW energy, highlighting the Hfq system with both RNA and ATP having poor value.

Table 3
Tabulation of average van der Waals energy (kcal/mol) calculated for eight systems.

S. No.	Systems	Van der waal's energy (kcal/mol)
1	Hfq (apo)	−78.673
2	Hfq + RNA	−67.155
3	Hfq + ATP	−70.276
4	Hfq + ATP + RNA	−49.723
5	Hfq(Y25A)	−75.456
6	Hfq(Y25A) + RNA	−61.820
7	Hfq(Y25A) + ATP	−67.665
8	Hfq(Y25A) + ATP + RNA	−72.257

4. Conclusions

Our earlier published works on *S. aureus* Hfq protein revealed the effect of few highly conserved, structurally and functionally important residues far from the nucleotide binding portion on RNA binding [24] and influence of high ionic salt concentration on Hfq–RNA binding conformation using molecular modeling studies [25]. In this study, considering Arluison et al.'s electron microscopic evidence on the overall six-fold symmetry of Hfq hexamers, we looked for the most favorable ATP binding site in Hfq and assessed its stability in the presence and absence of RNA. Moreover, we tested the importance of Tyr25 in Hfq for ATP binding and Hfq function by performing a hexamutant study on that residue with the modeled Hfq systems. Altogether, eight MD simulated systems were introduced: four wild-type Hfq systems, one each in the presence/absence of RNA and/or ATP, and four similarly configured hexamutant Hfq (Y25A) systems. Based on our study and applied computational methodologies, we were able to successfully obtain a stable and favorable ATP binding site in Hfq. Favorable π–π stacking interactions between the adenine ring of ATP and the Tyr25 ring were observed in our modeled systems.

During the course of the MD simulations, the Hfq systems bound to RNA were found to have moderately more protein backbone deviation and less protein compactness than the other modeled wild-type and hexamutant systems. We observed an increase in RNA pore diameter to 2 nm in all the hexamutant systems, which is essential for threading of RNA through it for the post-translational modification process. The presence of RNA tends to affect ATP binding in the wild-type systems. At around 4 ns, the ATP was found to lose its interaction with Hfq in presence of RNA. However, no effect of RNA on ATP binding was observed with hexamutant Hfq. Weak van der Waals interactions exist between the monomers in the Hfq + RNA + ATP system. Presumably, the six-fold symmetry of the Hfq ring might have broken in the presence of both RNA & ATP. These results can be interpreted as substantiating the electron microscopic work of Arluison et al., which states that the presence of both ATP and RNA disrupt Hfq's six-fold ring symmetry. The unstable behavior of the Tyr25Ala mutant systems reveals the importance of that residue for the proper ATPase mechanism of Hfq.

Our study indicates that the binding of both RNA and ATP is accompanied by a detectable distortion in the six-fold symmetry of Hfq. Such an alteration would not be possible without a significant conformational change in Hfq. Although the exact nature of this conformational change remains to be determined, our data and the corresponding results point to one of its functional structural consequences.

Acknowledgements

This research was supported by the Basic Science Research Program (2009-0073267), the Pioneer Research Center Program (2009-0081539), and the Environmental Biotechnology National Core Research Center program (20090091489) through the National Research Foundation of Korea (NRF) funded by the Ministry of Education, Science and Technology (MEST). All the students were recipients of fellowships from the BK21 Program of MEST.

References

[1] M.V. Sukhodolets, S. Garges, Interaction of *Escherichia coli* RNA polymerase with the ribosomal protein S1 and the Sm-like ATPase Hfq, Biochemistry 42 (2003) 8022–8034.
[2] R.G. Brennan, T.M. Link, Hfq structure function and ligand binding, Curr. Opin. Microbiol. 10 (2007) 125–133.
[3] E. Hajnsdorf, P. Reĭgnier, Host factor HFq of *Escherichia coli* stimulates elongation of poly (A) tails by poly (A) polymerase I, Proc. Natl. Acad. Sci. U.S.A. 97 (2000) 1501–1505.
[4] J. Le Derout, M. Folichon, F. Briani, G. Deho', P. Reĭgnier, F. Hajnsdorf, Hfq affects the length and the frequency of short oligo(A) tails at the 3¢ end of *Escherichia coli* rpsO mRNAs, Nucleic Acids Res. 31 (2003) 4017–4023.
[5] T. Blumenthal, G.G. Carmichael, RNA replication: function and structure of Qβ-replicase, Annu. Rev. Biochem. 48 (1979) 525–548.
[6] N. Majdalani, C.K. Vanderpool, S. Gottesman, Bacterial small RNA regulators, Crit. Rev. Biochem. Mol. 40 (2005) 93–113.
[7] T. Moller, T. Franch, P. Hojrup, D.R. Keene, H.P. Bachinger, R.G. Brennan, P. Valentin-Hansen, Hfq: a bacterial Sm-like protein that mediates RNA–RNA interaction, Mol. Cell 9 (1) (2002) 23–30.
[8] A. Zhang, K.M. Wassarman, J. Ortega, A.C. Steven, G. Storz, The Sm-like Hfq protein increases OxyS RNA interaction with target mRNAs, Mol. Cell 9 (1) (2002) 11–22.
[9] V. Arluison, S.K. Mutyam, C. Mura, S. Marco, M.V. Sukhodolets, Sm-like protein Hfq: location of the ATP-binding site and the effect of ATP on Hfq–RNA complexes, Protein Sci. 16 (9) (2007) 1830–1841.
[10] G. Jones, P. Willett, R.C. Glen, A.R. Leach, R. Taylor, Development and validation of a genetic algorithm for flexible docking, J. Mol. Biol. 267 (1997) 727–748.
[11] C. Sauter, J. Basquin, D. Suck, Sm-like proteins in Eubacteria: the crystal structure of the Hfq protein from *Escherichia coli*, Nucleic Acids Res. 31 (14) (2003) 4091–4098.
[12] M.A. Schumacher, R.F. Pearson, T. Møller, P. Valentin-Hansen, R.G. Brennan, Structures of the pleiotropic translational regulator Hfq and an Hfq–RNA complex: a bacterial Sm-like protein, EMBO J. 21 (13) (2002) 3546–3556.
[13] Discovery Studio 2.0 User Guide, Accelrys Inc. San Diego, CA, USA (2005), www.accelrys.com.
[14] H.J C. Berendsen, D. van der Spoel, R. van Drunen, GROMACS: a message-passing parallel molecular dynamics implementation, Comput. Phys. Commun. 91 (1995) 43–56.
[15] D. van der Spoel, E. Lindahl, B. Hess, G. Groenhof, A.E. Mark, H.J.C. Berendsen, GROMACS: fast flexible, and free, J. Comput. Chem. 26 (2005) 1701–1718.
[16] J. Eric Sorin, S. Vijay Pande, Exploring the helix-coil transition via all-atom equilibrium ensemble simulations, Biophys. J. 88 (2005) 2472–2493.
[17] W.L. Jorgensen, J. Chandrasekhar, J.D. Madura, R.W. Impey, M.L. Klein, Comparison of simple potential functions for simulating liquid water, J. Chem. Phys. 79 (1983) 926–935.
[18] U. Essman, L. Perela, M.L. Berkowitz, T. Darden, H. Lee, L.G. Pedersen, A smooth particle mesh Ewald method, J. Chem. Phys. 103 (1995) 8577–8592.
[19] H.J.C. Berendsen, J.P.M. Postma, A. Di Nola, J.R. Haak, Molecular dynamics with coupling to an external bath, J. Chem. Phys. 81 (1984) 3684–3690.
[20] M. Parrinello, A. Rahman, Polymorphic transition in single crystals: a new molecular dynamics method, J. Appl. Phys. 52 (1981) 7182–7190.
[21] B. Hess, H. Bekker, H.J.C. Berendsen, J.G.E. Fraaije, LINCS: a linear constraint solver for molecular simulations, J. Comput. Chem. 18 (1997) 1463–1472.
[22] J.P. Ryckaert, G. Ciccotti, H.J.C. Berendsen, Numerical integration of the Cartesian equations of motion of a system with constraints: molecular dynamics of n-alkanes, J. Comput. Phys. 23 (1977) 327–341.
[23] A.C. Wallace, R.A. Laskowski, J.M. Thornton, LIGPLOT: a program to generate schematic diagrams of protein–ligand interactions, Protein Eng. 8 (1995) 127–134.
[24] P. Lazar, S. Kim, Y. Lee, M. Son, H.-H. Kim, Y.S. Kim, K.W. Lee, Molecular modeling study on the effect of residues distant from the nucleotide binding portion on RNA binding in *Staphylococcus aureus* Hfq, J. Mol. Graph. Model 28 (2009) 253–260.
[25] P. Lazar, Y. Lee, S. Kim, M. Chandrasekaran, K.W. Lee, Molecular dynamics simulation study for ionic strength dependence of RNA-host factor interaction in *Staphylococcus aureus* Hfq, Bull. Korean Chem. Soc. 31 (2010) 1519–1526.